WK.2 Orthorhombic Distortion of Mismatched $In_xGa_{1-x}As$/InP Heterostructures

Brian R. Bennett and Jesús A. del Alamo

Massachusetts Institute of Technology, Cambridge, MA 02139

Thin, mismatched epilayers tetragonally distort to form coherent interfaces. Beyond the critical thickness, misfit dislocations relieve strain. These dislocations form in an asymmetric pattern on (001) zinc-blende substrates. We show that this results in a change of crystal symmetry from tetragonal to orthorhombic for partially relaxed, mismatched $In_xGa_{1-x}As$ epilayers in either tension or compression on InP. This distortion is detected by both double-crystal x-ray diffraction and ellipsometry.

INTRODUCTION

Ternary alloys of $In_xGa_{1-x}As$ are of growing interest for both electronic and optical devices. Much work has focussed on the alloy $In_{0.53}Ga_{0.47}As$ because it can be grown lattice-matched to InP substrates. The use of mismatched epitaxial layers, however, allows much greater freedom to design heterostructure devices with desired optical and electronic properties. For example, lattice mismatch can be introduced to achieve higher electron mobility and conduction band offset in InGaAs/InAlAs/InP field-effect transistors[1].

If the mismatch between the epilayer and substrate is small and the layer is thin, the mismatch will be accomodated entirely by strain in the layer. In this case, the symmetry of the epilayer lattice distorts from cubic to tetragonal (Poisson effect). For layers exceeding the critical layer thickness[2], the formation of misfit dislocations at the epilayer/substrate interface becomes energetically favorable. These dislocations relieve strain, allowing the epilayer lattice to relax back toward cubic symmetry. In the case of zinc-blende semiconductors such as InP and InGaAs, misfit dislocations form in an asymmetric network on (001) substrates[3-5]. Specifically, dislocations first form along the $[1\bar{1}0]$ direction, and then in the orthogonal [110] direction. This should result in a change of crystal symmetry from tetragonal to orthorhombic before the layer relaxes to cubic symmetry for very large mismatches or thick epilayers.

EXPERIMENTAL PROCEDURES

For this study, we grew single epitaxial layers of $In_xGa_{1-x}As$ on semi-insulating (001) InP substrates, using a Riber model 2300 solid-source molecular beam epitaxy (MBE) system. The substrate temperature, measured by a thermocouple and optical pyrometer, was about 500°C. The V:III ratio was 15-25, and the growth rates ranged from 0.6 to 0.9 μm/hr.

All the samples were characterized by DCXRD to determine layer composition and strain. The rocking curves were measured by either a Bede model 150 or model 300 system with Cu-Kα radiation and an InP first crystal oriented for the (004) reflection. Rocking curves were measured for symmetric (004) reflections as well as asymmetric (115) and (224) reflections. For selected samples, DCXRD measurements were made as a function of azimuthal angle, α, as shown in fig. 1. We define $\alpha = 0$ when the projection of the incident beam on the wafer surface is in the [110] direction.

We measured the optical properties of the layers with a Gaertner model L116B automated ellipsometer. Both circularly and linearly polarized incident light from a He-Ne laser ($\lambda = 0.633\ \mu$m) were used with the angle of incidence fixed at 70° from vertical. The ellipsometer measures the polarization ellipse of the reflected light. From this, the parameters Δ and ψ are calculated. Δ is the phase difference in the TM and TE reflected waves, and ψ is the arctangent of their amplitude ratio. Measurements were made as a function of azimuthal angle (see fig. 1). We refer to this technique as variable azimuthal angle ellipsometry (VAAE)[6].

RESULTS AND DISCUSSION

1. Symmetric Double-Crystal X-Ray Diffraction

For symmetric geometries such as (004) reflections on (001) substrates, the separation between the substrate and epitaxial peaks, $\Delta\theta$, is a function of only the mismatch in lattice constant perpendicular to the interface, $(\Delta a/a)_\perp$. In fig. 2, we show DCXRD (004) data for sample 1605, a 1000 Å layer of $In_{0.44}Ga_{0.56}As$ on InP, measured at azimuthal angles of 0 and 90°. The peak separation is identical within experimental error for the two curves, yielding a perpendicular mismatch of -1.25 x 10^{-3}, where the negative sign indicates an epilayer in tension. Note, however, that the full width at half maximum (FWHM) of the epilayer peaks are different for $\alpha = 0$ and 90°: 690 and 440 arc-seconds, respectively. In fig. 3, we plot the (004) FWHM as a function of azimuthal angle for nine rocking curves measured on sample 1605. The results approximately follow a cosine law, with FHWM minima at $\alpha = 90$ and 270°. We have observed this effect for epilayers in both compression and tension. The compression data follow the same pattern as in fig. 3.

Rocking curve epitaxial peaks can be broadened by both finite thickness effects and misfit dislocations. The theoretical FWHM's for 1000 and 1800 Å thick InGaAs layers are 170 and 95 arc-seconds, respectively[7]. Hence, we attribute the additional broadening in fig. 3 (FWHM's from 420 to 690 arc-seconds) to misfit dislocations which cause a local tilting of lattice planes. These tilted planes will satisfy the Bragg condition at angles that differ slightly from the Bragg angle for a dislocation-free layer. If the number of dislocations along the $[1\bar{1}0]$ direction exceeds the number along [110] (as schematically illustrated in fig. 1) the peak width observed along [110] ($\alpha = 0°$) should be greater than that observed along $[1\bar{1}0]$ ($\alpha = 90°$), as our experiments indicate. Such an anisotropic dislocation density distribution has been observed by Grundmann *et al.* for InGaAs/GaAs heterostructures[8]. We conclude that the (004) DCXRD data of fig. 3 demonstrates asymmetric lattice relaxation along the [110] and $[1\bar{1}0]$ directions in the InGaAs epilayer. Direct measurements of lattice relaxation are presented in the next section.

2. Asymmetric Double-Crystal X-Ray Diffraction

If a mismatched layer is below the critical thickness, the lattice will be completely continuous across the interface and the mismatch in lattice constant parallel to the interface, $(\Delta a/a)_{\parallel}$, will be zero. The layer is said to be coherent. For layers exceeding the critical thickness, misfit dislocations may form at the epilayer/substrate interface, resulting in a non-zero $(\Delta a/a)_{\parallel}$ and a partially relaxed layer. Hence, measurement of both $(\Delta a/a)_{\parallel}$ and $(\Delta a/a)_{\perp}$ is necessary to characterize an epilayer. This is accomplished by measuring the rocking curves for asymmetric reflections such as (115) and (224). For (001) substrates, these planes will not be parallel to the surface, and $\Delta\theta$ will be a function of both $(\Delta a/a)_{\parallel}$ and $(\Delta a/a)_{\perp}$. If $(\Delta a/a)_{\perp}$ is known from an (004) measurement, $(\Delta a/a)_{\parallel}$ can be estimated from a single asymmetric rocking curve.

Since misfit dislocations relieve epilayer strain, an asymmetry in misfit dislocation density should result in different parallel lattice mismatches in the orthogonal [110] and $[1\bar{1}0]$ directions, as has been observed in III-V heterostructures[9,10]. We observe it for our InGaAs/InP heterostructures in both tension and compression. An example is given in fig. 4, which shows (224) rocking curves for sample 1442, 3000 Å of $In_{0.66}Ga_{0.34}As$. The peak separation, $\Delta\theta$, is different for the curves measured at $\alpha = 0$ and 90°. To calculate the parallel mismatches, we average scans separated by 180° [$(\Delta a/a)_{\parallel[110]}$ is calculated from the average of $\Delta\theta_{(224)}$ ($\alpha = 0°$) and $\Delta\theta_{(224)}$ ($\alpha = 180°$); $(\Delta a/a)_{\parallel[1\bar{1}0]}$ is calculated from the average of $\Delta\theta_{(224)}$ ($\alpha = 90°$) and $\Delta\theta_{(224)}$ ($\alpha = 270°$)] to eliminate differences in $\Delta\theta$ caused by epilayer tilt. An epilayer lattice may now be characterized by three mismatches: $(\Delta a/a)_{\perp}$, $(\Delta a/a)_{\parallel[110]}$, and $(\Delta a/a)_{\parallel[1\bar{1}0]}$. The relaxed lattice constant is then defined by:

$$\left(\frac{\Delta a}{a}\right)_r = \frac{1-\nu}{1+\nu}\left(\frac{\Delta a}{a}\right)_{\perp} + \frac{\nu}{1+\nu}\left[\left(\frac{\Delta a}{a}\right)_{\parallel[110]} + \left(\frac{\Delta a}{a}\right)_{\parallel[1\bar{1}0]}\right] \quad (1)$$

where ν is Poisson's ratio. If $(\Delta a/a)_{\perp} \neq (\Delta a/a)_{\parallel[110]} \neq (\Delta a/a)_{\parallel[1\bar{1}0]}$, the distortion is orthorhombic. For example, the data for sample 1442 of fig. 4 indicates that $(\Delta a/a)_{\perp} = 10.4 \times 10^{-3}$, $(\Delta a/a)_{\parallel[110]} = 8.6 \times 10^{-3}$, and $(\Delta a/a)_{\parallel[1\bar{1}0]} = 5.4 \times 10^{-3}$. Using $\nu = 1/3$, we find $(\Delta a/a)_r = 8.7 \times 10^{-3}$.

Whereas the degree of relaxation is defined by a single parameter in the case of purely tetragonal distortion[11], two parameters are needed to characterise orthorhombic distortion. We define:

$$R_{[110]} = \frac{\left(\frac{\Delta a}{a}\right)_{\parallel[110]}}{\left(\frac{\Delta a}{a}\right)_r} \quad (2)$$

$$R_{[1\bar{1}0]} = \frac{\left(\frac{\Delta a}{a}\right)_{\parallel[1\bar{1}0]}}{\left(\frac{\Delta a}{a}\right)_r} \quad (3)$$

We also define the average relaxation, $\bar{R}$, as $(R_{[110]} + R_{[1\bar{1}0]})/2$.

We have observed orthorhombic distortion in all of our heterostructures exhibiting significant relaxation ($\bar{R} > 0.1$). In fig. 5, we plot the difference in $R_{[110]}$ and $R_{[1\bar{1}0]}$ versus the average relaxation. For all samples, regardless of compression or tension, we find that $R_{[110]} > R_{[1\bar{1}0]}$. This indicates that a majority of misfit dislocations lie along the $[1\bar{1}0]$ direction, relieving strain in the [110] direction (see fig. 1). In fig. 5 the origin represents purely tetragonal distortion, whereas the point (1,0) corresponds to complete relaxation and cubic symmetry. The area above the x-axis represents orthorhombic distortion. Our data clearly indicates significant orthorhombic distortion for a wide range of relaxation.

In fig. 6 we show a schematic view of lattice distortion. We assume the epilayer has a larger lattice constant than the substrate. For layers less than the critical thickness ($t < t_c$), tetragonal distortion results (a). For $t > t_c$, misfit dislocations form in an asymmetric pattern, partially relaxing the strain and resulting in orthorhombic distortion (b). For $t >> t_c$, the strain is fully relieved by dislocations and the epilayer symmetry is cubic (c).

3. Variable Azimuthal Angle Ellipsometry

Ellipsometry also reveals orthorhombic distortion when the layer is examined as a function of azimuthal angle[6]. In fig. 7, we plot the ellipsometric parameter Δ as a function of asimuthal angle for sample 1605. The results follow a cosine law, and can be very precisely fit by the function:

$$\Delta = A_\Delta + B_\Delta \cos[2(\alpha - C_\Delta)] \quad (4)$$

All of our samples show a Δ vs. α pattern similar to fig. 8, although the amplitude of the cosine function, B_Δ, varies substantially. This is illustrated in fig. 8 where we plot B_Δ as a function of the magnitude of the lattice mismatch for samples in compression and tension. The samples are coded based upon the average relaxation measured by DCXRD. For $|(\Delta a/a)_r| \leq 2 \times 10^{-3}$, B_Δ is small, suggesting little or no orthorhombic distortion. As $|(\Delta a/a)_r|$ increases, B_Δ also increases, reaching values of 5-10°. The samples with significant relaxation, however, have smaller values of B_Δ. The relaxed samples in fig. 8 are the samples in which we directly detected asymmetric relaxation (fig. 5).

4. Comparison of Methods

All three characterization methods show evidence of orthorhombic distortion for epilayers in both tension and compression. All techniques also show that the direction of dominant relaxation is the same in tension and compression: in the case of VAAE, B_Δ is always positive; asymmetric DCXRD always shows $(\Delta a/a)_{\|[110]} > (\Delta a/a)_{\|[1\bar{1}0]}$; the (004) (symmetric) DCXRD FWHM always have minima at $\alpha = 90, 270°$. We conclude that the misfit dislocations first form along the $[1\bar{1}0]$ direction, regardless of the sign of the strain.

Asymmetric DCXRD did not detect relaxation on the five samples with the largest B_Δ's (fig. 8) These results suggest that VAAE is able to detect orthorhombic distortion sooner than asymmetric DCXRD although the range of DCXRD could improve if extremely long count times are used in x-ray systems with low background. VAAE has the advantages of safety and speed: a complete set of measurements such as fig. 8 can be taken in 5-10 minutes. It is, however, a very new technique and the ability to determine epilayer strains directly from VAAE data has not yet been demonstrated.

ACKNOWLEDGEMENTS

This work was funded by a Fellowship from the Air Force Office of Scientific Research/Rome Laboratories (BRB) and a grant from NTT Corporation (JdA). The authors thank Prof. C.G. Fonstad for the use of his MBE.

REFERENCES

[1] W.-P. Hong *et al.*, *J. Appl. Phys.* **64**, 1945 (1988).
[2] J.W. Matthews and A.E. Blakeslee, *J. Crystal Growth* **27**, 118 (1974).
[3] M.S. Abrahams *et al.*, *J. Mater. Sci.* **4**, 223 (1969).
[4] E.A. Fitzgerald *et al.*, *J. Appl. Phys.* **65**, 2220 (1989).
[5] S.R. Bahl, W.J. Azzam, and J.A. del Alamo, *J. Crystal Growth*, to be published (1991).
[6] B.R. Bennett and J.A. del Alamo, *Mat. Res. Soc. Symp. Proc.* **160**, 713 (1990).
[7] X-ray simulation program RADS from Bede Scientific.
[8] M. Grundmann *et al.*, *Appl. Phys. Lett.* **55**, 1765 (1989).
[9] K.S. Kavanagh, *et al.*, *J. Appl. Phys.* **64**, 4843 (1988).
[10] A.G. Turnbull *et al.*, *Mat. Res. Soc. Symp. Proc.* **202**, to be published (1991).
[11] M.A.G. Halliwell, *Adv. X-ray Anal.* **33**, 61 (1990).

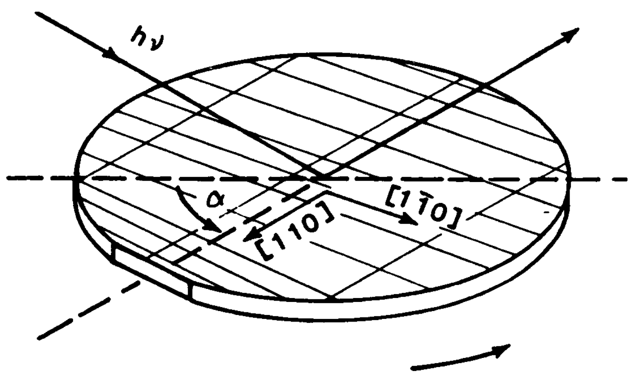

Fig. 1: Geometry of x-ray and ellipsometry measurements; α is the asimuthal angle (angle of rotation) of the projection of the beam on the sample with respect to the [110] direction. An asymmetric array of misfit dislocations is also shown.

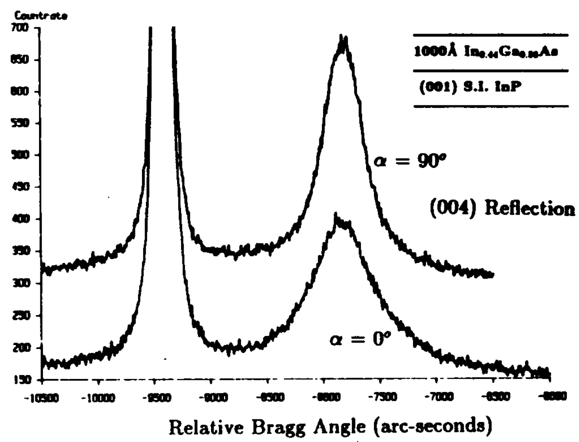

Fig. 2: (004) DCXRD rocking curves for sample 1605, showing different epilayer peak widths at $\alpha = 0$ and 90°. The 90° curve is shifted up for clarity.

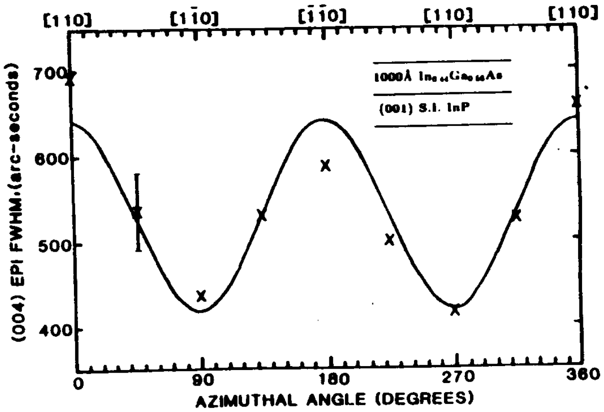

Fig. 3: (004) DCXRD epilayer peak width as a function of azimuthal angle for sample 1605 (epilayer in tension). Solid line is a least-squares fit to a cosine function.

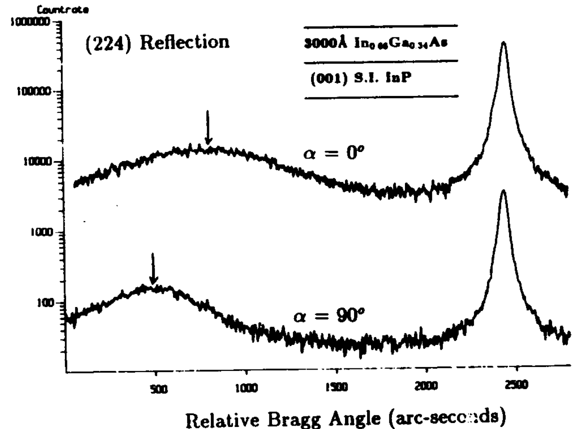

Fig. 4: DCXRD rocking curves for (224) reflections of sample 1442 at azimuthal angles of 0° and 90°. The 0° curve is shifted up by a factor of 100 for clarity.

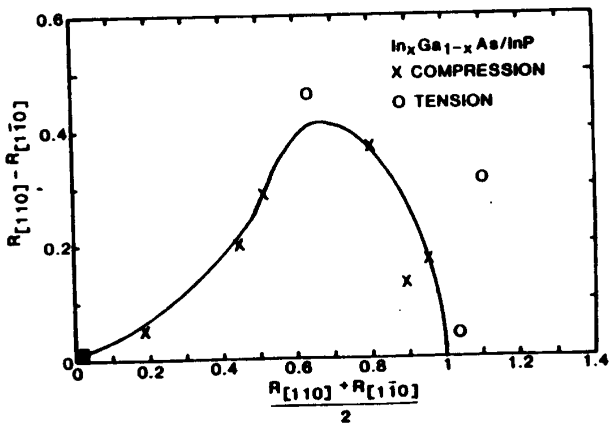

Fig. 5: Difference in relaxation in the [110] and [1$\bar{1}$0] directions as a function of average relaxation for nine partially relaxed epilayers.

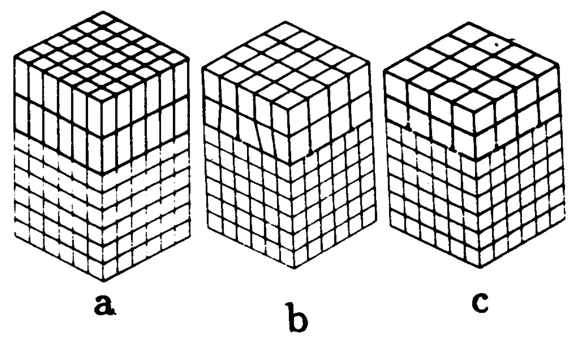

Fig. 6: Schematic view of lattice distortion as a function of degree of relaxation for epilayer with larger lattice constant than substrate (see discussion in test).

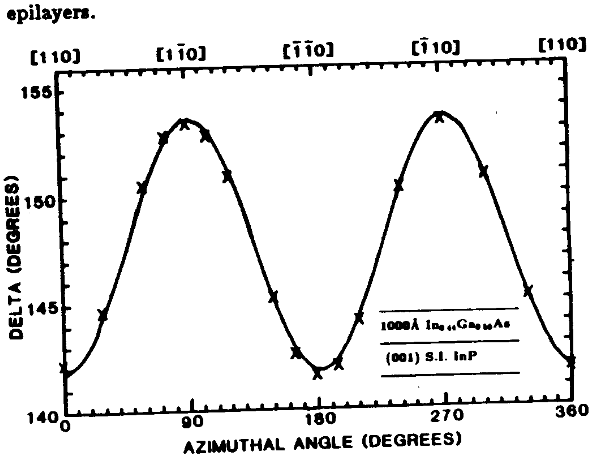

Fig. 7: Ellipsometric parameter Δ as a function of azimuthal angle for sample 1605. Solid line is a least-squares fit to eqn. (4).

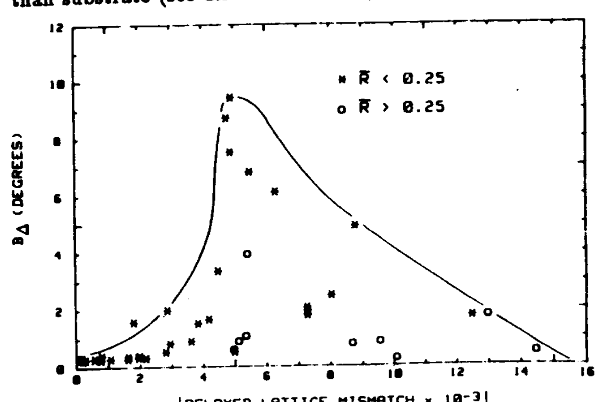

Fig. 8: The amplitude of the cosine function fits for the ellipsometric parameter Δ as a function of the magnitude of the lattice mismatch. Samples (in both compression and tension) are coded by average layer relaxation.